

CFD AND EXPERIMENTAL STUDY OF AERODYNAMIC DEGRADATION OF ICED AIRFOILS

Vladimír Horák¹, Dalibor Rozehnal², Zdeněk Chára³, Andrej Hyll¹

¹Department of Mechanical Engineering, University of Defence, Brno

²Department of Aerospace and Rocket Technologies, University of Defence, Brno

³Institute of Hydrodynamics, AS CR, v. v. i., Prague

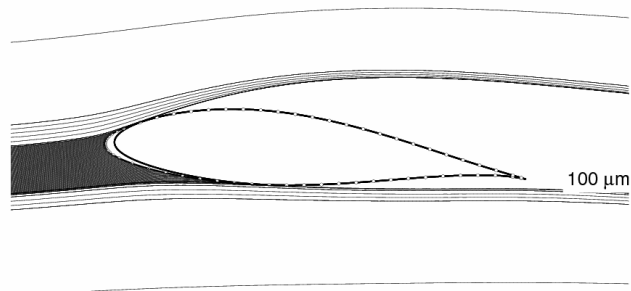
1. Introduction

The phenomenon of in-flight icing may affect all types of aircraft. The formation of ice on wings occurs when the aircraft flies at a level where temperature is at, or below freezing point and hits super-cooled water droplets. Presence of ice accretion on wings and other aircraft components can lead to a number of aerodynamic degradation problems and consequently is a major problem of safety. From aerodynamics viewpoint, when compared to wings without ice, wings with ice indicate decreased maximum lift, increased drag, changes in pressure distribution, stall occurring at much lower angles of attack, increased stall speed, and reduced controllability [1]. Thus, it is important to understand the different ice shapes that can form on the wings and how they affect aerodynamics. It can be studied by flight tests, wind tunnel measurements, and computational simulations. Flight tests are the most realistic but are expensive. Tests in icing wind tunnels offer a controlled environment, but cannot reproduce actual flight conditions since not all dimension-less parameters can be matched. Computational simulation is the most cost effective method. However, its accuracy depends on the ability to reproduce the key flow physics.

2. Ice Accretion Prediction Code

In conjunction with the project of the Czech Ministry of Industry and Trade, was developed the tool for simulating flight into icing conditions. R-ICE is an ice accretion prediction code [2] that applies a time-stepping procedure to calculate the shape of an ice accretion. The potential flow field is calculated in R-ICE using 2-D panel code. This potential flow field is then used to calculate the trajectories of water droplets and the impingement points on the body. Droplets passing through the atmosphere are considered as spherical shape elements on that the surrounding fluid forces (aerodynamic and aerostatic) and gravitation act. Typical results of droplets trajectories solution near an airfoil are shown in Fig. 1.

Fig. 1. Illustration of the water droplets trajectories. Airfoil NACA 633 418, water content $1 \text{ g}\cdot\text{m}^{-3}$, velocity $50 \text{ m}\cdot\text{s}^{-1}$, angle of attack 5° .



Mentioned R-ICE software was subsequently developed and modified. Actually enables to simulate both basic kinds of ice that can be formed on the wing surface: the *rime ice* if all the impinging super-cooled water droplets freeze immediately upon impact and the *glaze ice*, if not all of the impinging water freezes on impact, the thin layer of remainder water is flowing along the surface and freeze at other locations. The latest code version [3] enables the icing simulation of multi-element airfoils (e.g. airfoil with slotted flap, wing slot, etc.), when the mutual flow overlap of circumfluent bodies can occur.

Although the R-ICE code was primarily developed as a tool for study and prediction of airfoil ice accretion, the code provides a number of data and graphical output files. Among them is an output file of airfoil pressure distribution coefficient. An example of the graphical output file of the pressure coefficient c_p is shown in Fig. 2.

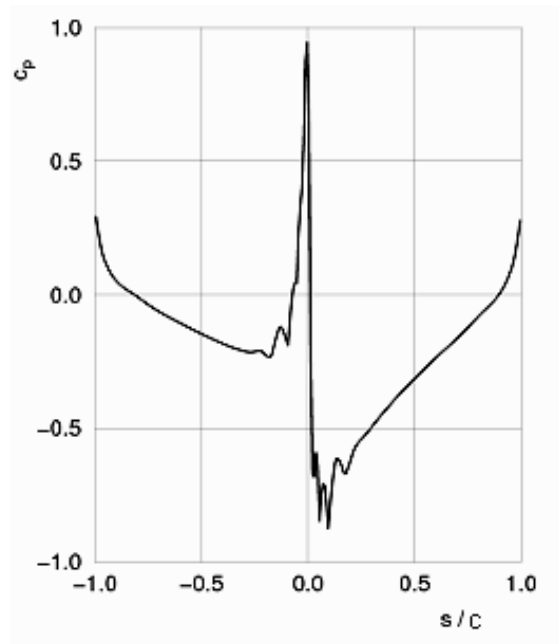


Fig. 2. Example of pressure coefficient c_p on dimensionless airfoil surface length s/c . Clean airfoil NACA 0012, chord $c = 0.1$ m, velocity $20 \text{ m}\cdot\text{s}^{-1}$, angle of attack 2° .

The pressure distribution round the airfoil can be utilized for aerodynamic characteristics determination. It is simply possible to compute the basic aerodynamics characteristic from the airfoil pressure distribution. Results of the lift coefficient solution in dependence on angle of attack, for NACA 0012 airfoil, chord $c = 0.1$ m and free stream velocity $20 \text{ m}\cdot\text{s}^{-1}$ are plotted in Fig. 3. There are outlined results for two different ice shapes chosen from available experimental data [4]. The first case is the mixed rounded ice shape C5 and the second one is the glaze horn ice shape C17. Drawings of the mentioned iced airfoils geometry are shown in comparison with the clean airfoil in Fig. 3, too.

The resulting characteristics are typical for a symmetric airfoil. It is evident that the aerodynamic behavior of iced and clean airfoil is similar. This is because the iced airfoils keep as geometrically close to the original clean airfoil shape. Differences are only round the leading edge.

Resulting courses of the lift coefficient solution neglect a stall as the used panel method is not able to involve the effect of stall, influence of which is critically important.

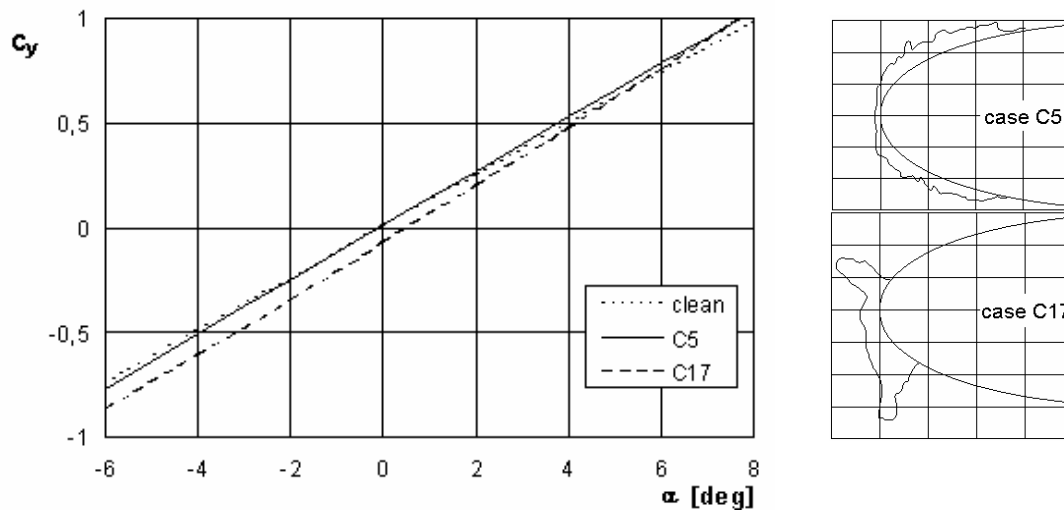


Fig. 3. Results of lift coefficient in dependence on angle of attack for NACA 0012 airfoil.

3. Iced Airfoil Wind Tunnel Testing

Results from icing wind tunnel and flight icing tests indicate [5] that the icing creates mainly nearby the airfoil leading edge. Therefore the wooden NACA0012 airfoil model was designed with the replaceable stereo-lithographical model of leading edge (Fig. 4). It enables the very simple ice shapes changing. Drawings of iced airfoils geometry mentioned above, photos of replaceable leading edges, and the photo of iced airfoil model with the replaceable leading edges are pictured in Fig. 4.

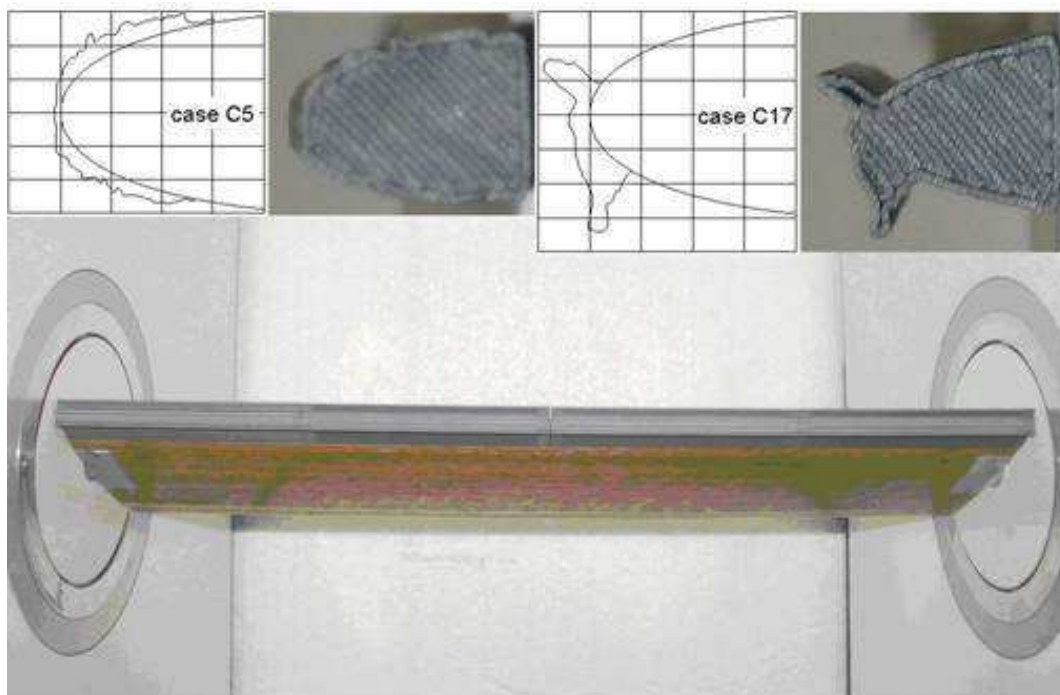


Fig. 4. Model of iced NACA0012 airfoil in the wind tunnel test section.

Iced airfoil wind tunnel testing was realized in the laboratory of aerodynamics at the Department of Aerospace and Rocket Technologies of the University of Defense. For the measurement of iced airfoils aerodynamic characteristics were used models with an artificial ice shapes for the wind tunnel experiments in dry air. The wind tunnel is the circulation one with a diameter of measuring space 600 mm. Measuring network covers mainly National Instrument device and software LAB-VIEW.

Results of outlined iced airfoils wind tunnel tests are plotted in Figures 5 and 6. Fig. 5 shows the effect of ice shape on the airfoil lift coefficient c_L in compare to the clean airfoil. It can be seen that ice shapes also cause both $c_{L,max}$ and α_{stall} . Fig. 6 shows the effect of ice shape on the airfoil drag coefficient c_D . Drag increases substantially for double horn glaze ice shape C17, especially at lower angles of attack.

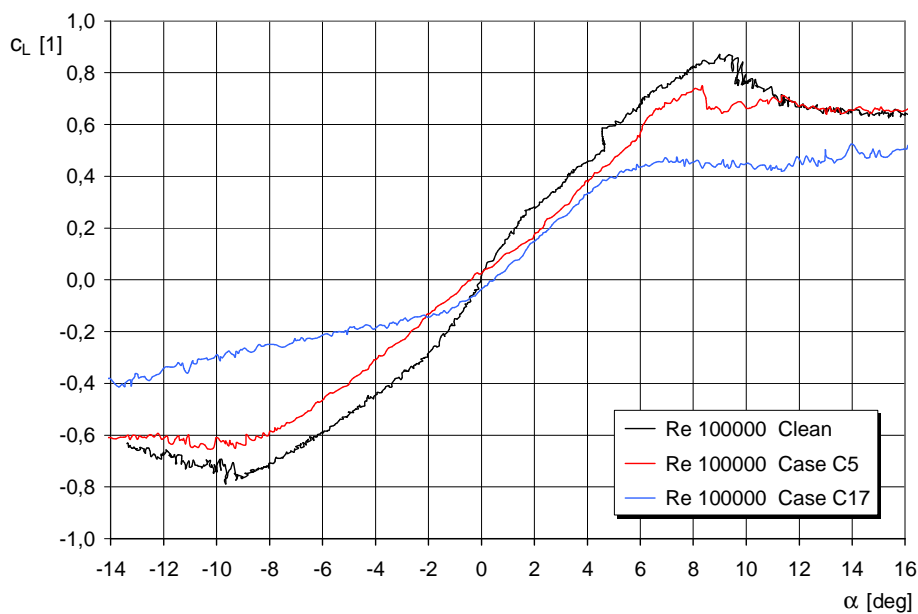


Fig. 5. Effect of ice shape on lift coefficient c_L for NACA0012 airfoil.

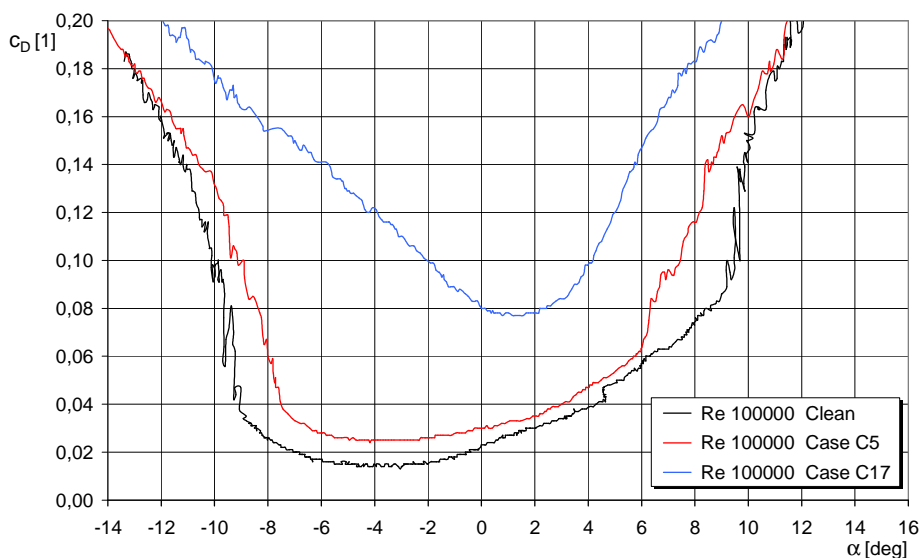


Fig. 6. Effect of ice shape on drag coefficient c_D for NACA0012 airfoil.

4. Two-Dimensional CFD Simulation

Regarding the fact that the panel method for the solution of a velocity distribution round a wing airfoil used in R-ICE code is not able to involve the effects of stall at higher angles of attack; it will have to be used two-dimensional CFD simulation to get more precise results. The CFD software ANSYS CFX 11.0 is available at University of Defence. The advanced fluid flow modeling is used to study aerodynamics of iced airfoils the geometry of whose is enormously complicated (Fig. 4).

A hybrid mesh was generated using the auto mesh generator ICEM CFD. The mesh was made of triangular elements of different sizes, while trapezoidal mesh is used in the boundary layer. The grid near the clean airfoil NACA 0012 airfoil surface is shown in Fig. 7.

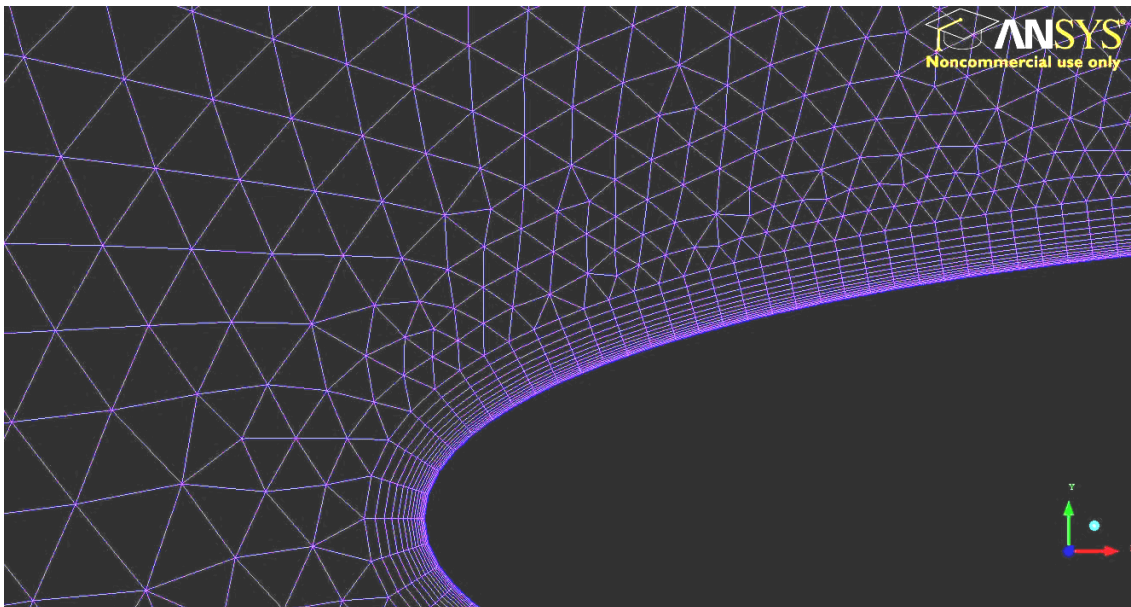


Fig. 7. Grid details near the airfoil surface.

The input parameters of simulation are the following:

- The ambient air temperature is 25 °C; fluid is of constant density and flows without heat transfer.
- Regarding the suitable mesh generation, the 1 m airfoil chord was chosen. Then the velocity is 2 m·s⁻¹ and the corresponding Reynolds number is 138 000, with respect to the similarity of the above flow regime.
- Low free stream turbulence intensity flow (1%) is considered.
- The wall shear stress transition onset follows gamma theta model.
- The change of angle of attack is obtained through a rotation of the coordinate frame.
- The calculation is stopped when the difference between two consecutive matrices (the residual target) reaches 10⁻⁵.

The program generates various output file formats. There are shown two examples of outputs in Figures 8 and 9. Fig. 8 shows the velocity distribution over the clean airfoil at an angle of attack of 8° .

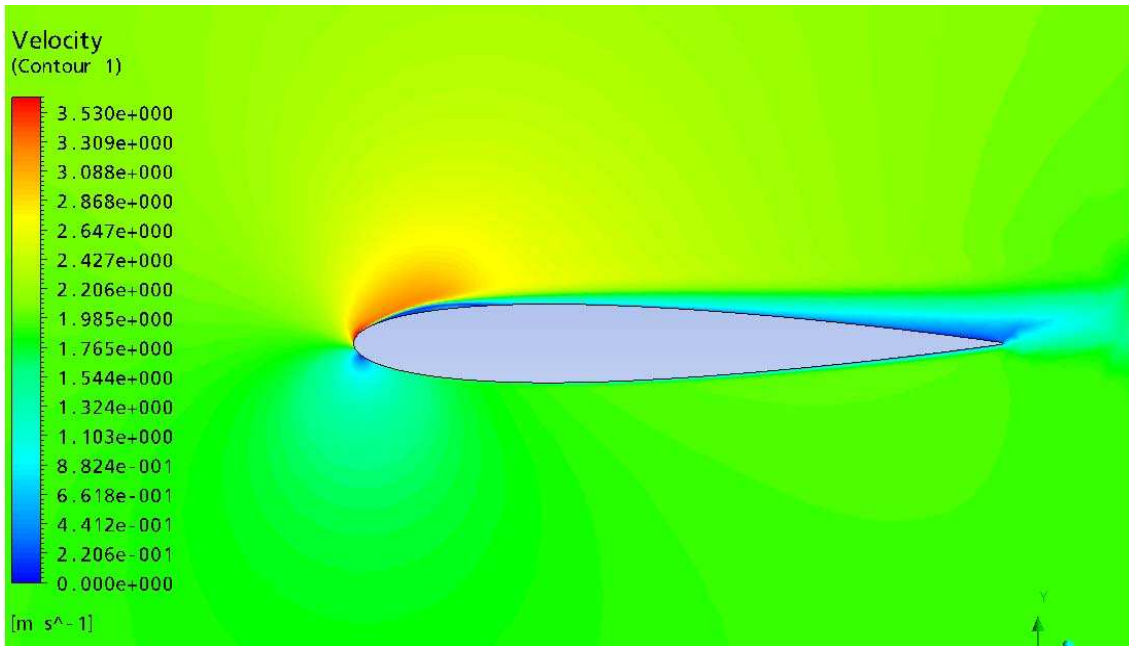


Fig. 8. Velocity distribution around the airfoil.

The transition effects are characterized by a laminar-turbulent intermittency. A sample plot of the turbulence intermittency near the airfoil is shown in Fig. 9.

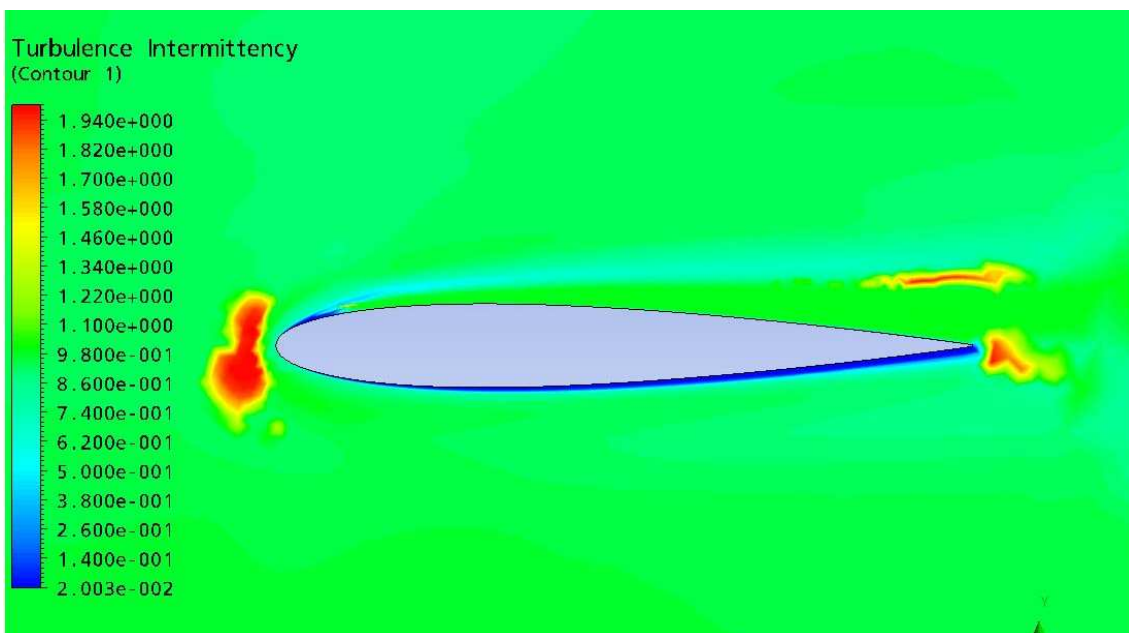


Fig. 9. Turbulence intermittency near the airfoil.

The pressure distribution around the airfoil is an important parameter in terms of integral aerodynamic characteristics, since it determines the lift coefficients of the airfoil. The example of pressure distribution around the airfoil NACA 0012 at $\alpha = 8^\circ$ is given in Fig. 10.

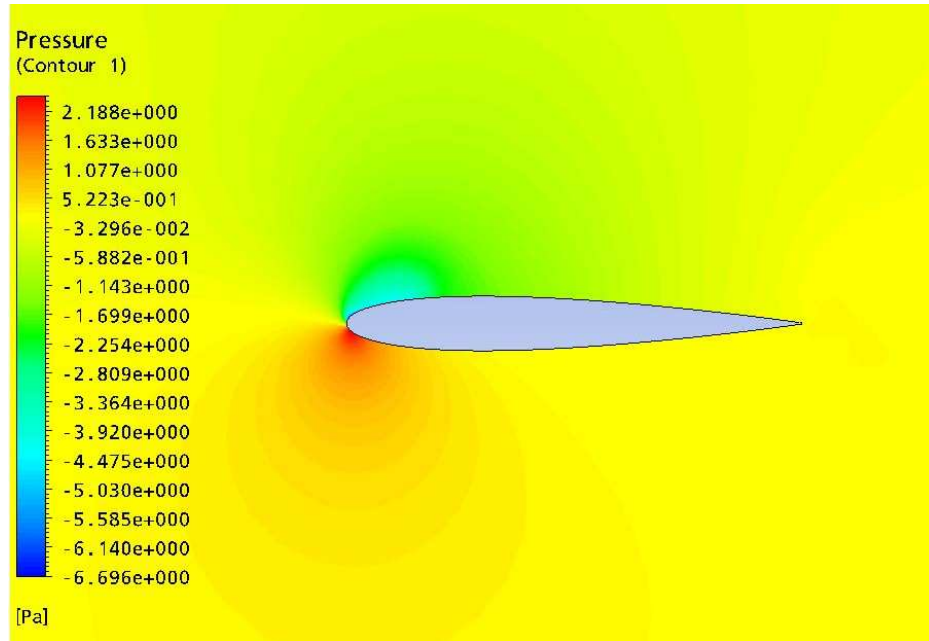


Fig. 10. Pressure distribution around the airfoil.

The lift coefficient c_L is given by the integration over the wall pressure distribution along the airfoil surface depicted in Fig. 11. The pressure scale is the same as in Fig. 10.

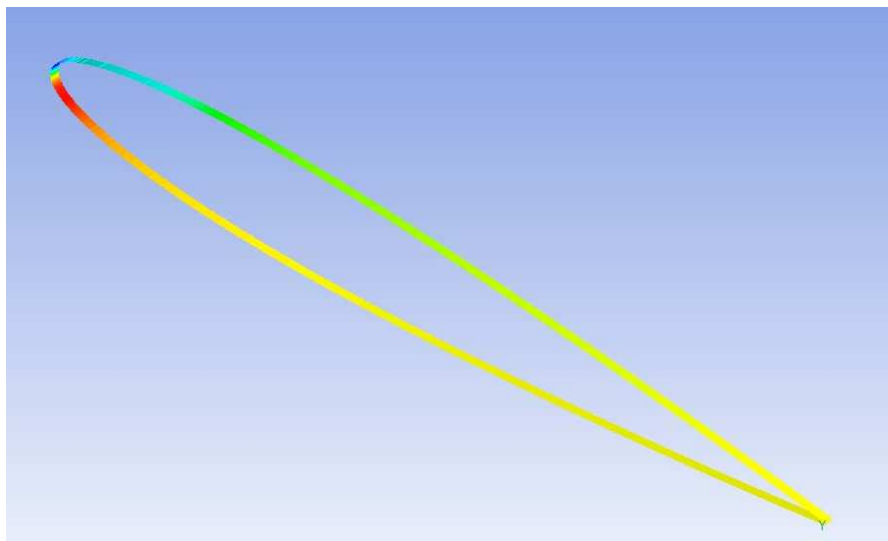


Fig. 11. Wall pressure distribution along the airfoil surface.

A CFD solution was performed for the airfoil ice accretion cases used in the experiment (Fig. 4). The lift coefficients c_L were computed with CFX 11.0 for angles of attack from -20° to 20° with 1 degree step for each case. The computed dependence of the lift coefficient at different angles of attack is shown in Fig. 12. There are compared lift curves for clean airfoil NACA 0012 and two cases of iced airfoils shapes C5 and C17.

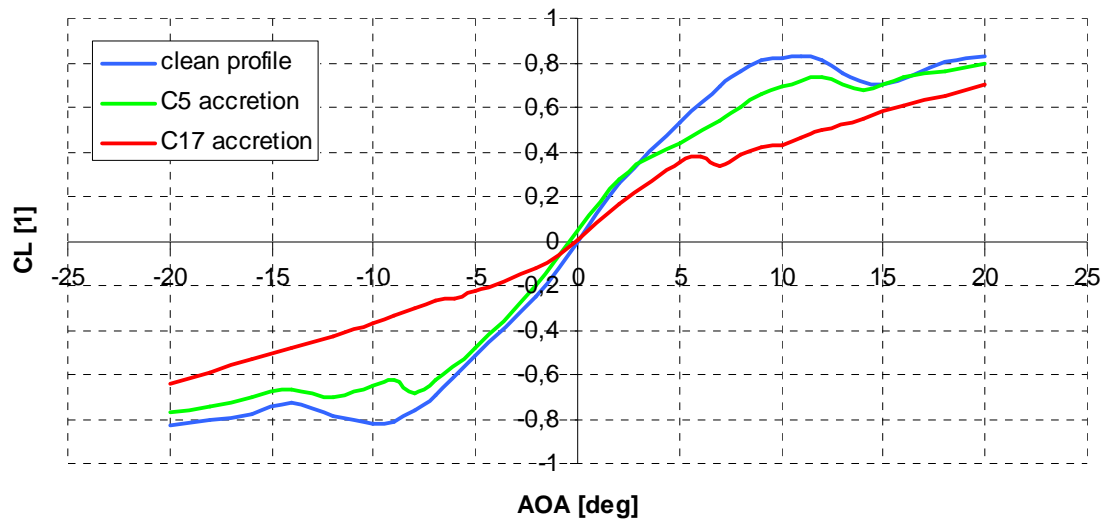


Fig. 12. Comparison of lift curves for clean airfoil and iced airfoils cases C5 and C17.

5. Conclusions

From the comparison in Fig. 12, the expected observations can be made: airfoils with ice indicate decreased maximum lift and the stall occurs at much lower angles of attack. This degradation influence is greater for the glaze horn ice shape C17.

The comparison of the above results of CFD solution with those obtained in the experiment is shown in Figures 13, 14, and 15 for clean airfoil NACA 0012 and iced airfoils cases C5 and C17. There are shown results of R-ICE panel method solution too.

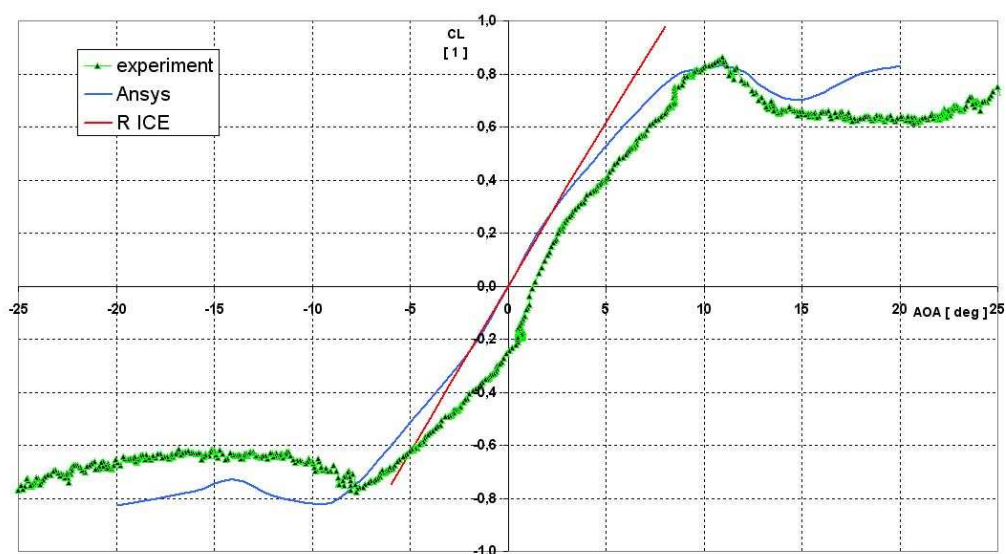


Fig. 13. Comparison of lift curves for clean airfoil NACA 0012.

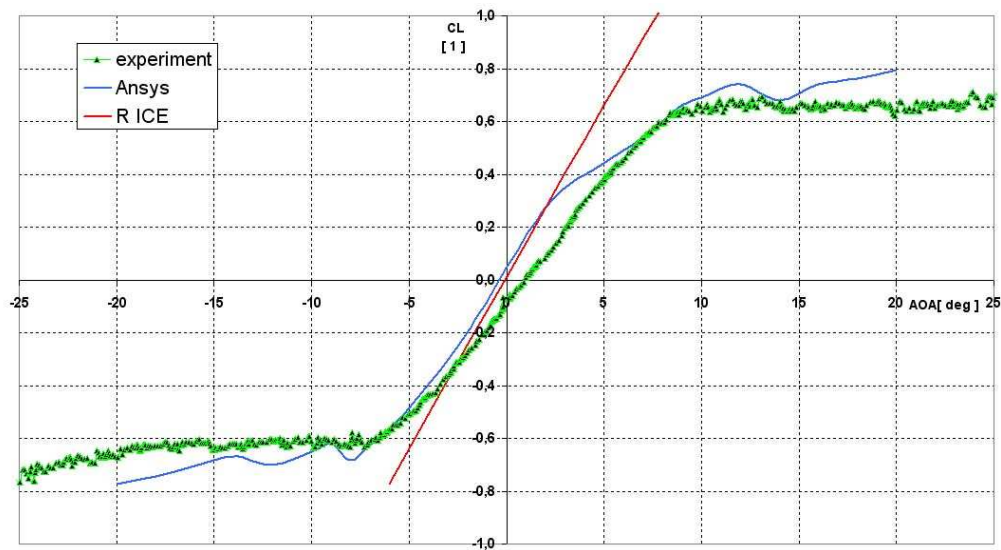


Fig. 14. Comparison of lift curves for iced airfoil case C5.

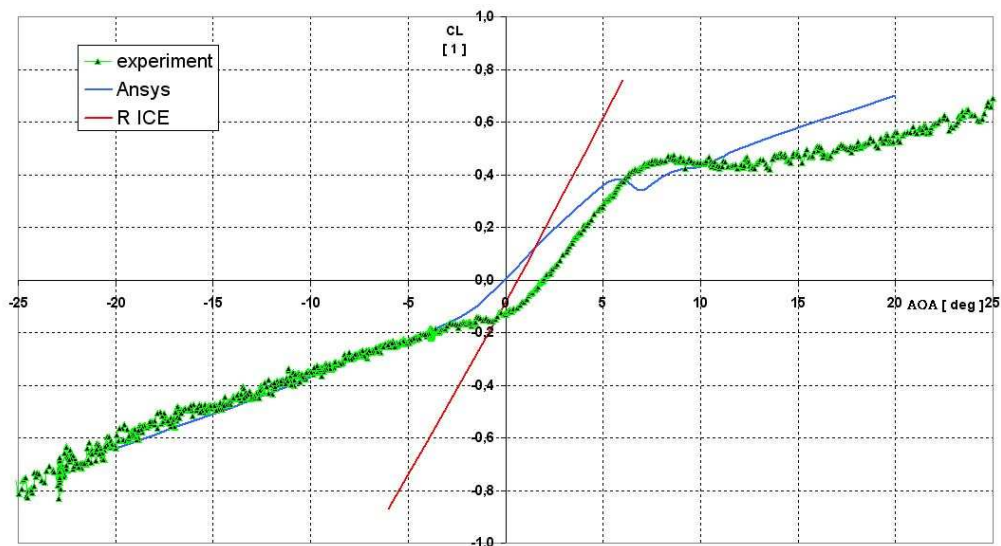


Fig. 15. Comparison of lift curves for iced airfoil case C17.

Comparing the lift curves for the above cases in Figures 13, 14, and 15, we can state a fairly good agreement between the results of the CFD simulation and experimentally obtained values.

On the contrary, the results of R-ICE panel method are useable for clean airfoils or rounded ice shapes (C5) and only for small angles of attack, up to $\pm 5^\circ$.

The CFD investigation provides a reasonable prediction of the lift curves of iced airfoils. But the computation of the aerodynamic drag coefficients by the CFD simulation generally does not give satisfactory results. Therefore, the wind tunnel testing has an irreplaceable role in the study of airfoil aerodynamics.

Acknowledgement

The work presented in this paper has been supported by the Czech Science Foundation (project No. 103/07/0136) and by the Czech Ministry of Industry and Trade (project FT-TA4/044 “InICE”).

References

- [1] I. Paraschivoiu and F. Saeed. *Aircraft Icing*. A Wiley-Interscience Publication, John Wiley & Sons, INC.
- [2] B. Hoření and V. Horák. *Users Manual for the Wing Airfoil Ice Accretion Code R-ICE, Version 1.1* (in Czech). Prague : Institute of Hydrodynamics, 2005, 27 p.
- [3] B. Hoření and V. Horák. *Users Manual for the Wing Airfoil Ice Accretion Code ICE, Version 3.1* (in Czech). Prague : Institute of Hydrodynamics, 2007, 34 p.
- [4] R. J. Kind. *Ice Accretion Simulation Evaluation Test*. RTO Technical Report 38, November 2001.
- [5] M. B. Bragg, A. P. Broeren, and L. A. Blumenthal. *Iced-Airfoil Aerodynamics*. Progress in Aerospace Sciences, Vol. 41, No.5, pp. 323-418, July 2005.